DOI: 10.13009/EUCASS2017-447

Wing geometric parameter studies of a box wing aircraft configuration for subsonic flight

Fábio Cruz Ribeiro*, Adson Agrico de Paula*, Dieter Scholz** and Roberto Gil Annes da Silva*
Instituto Tecnológico de Aeronáutica
Address: Instituto Tecnológico de Aeronáutica, Departamento de Projeto de Aeronaves. São José dos Campos, SP,12228900, Brasil.
** Hamburg University of Applied Sciences*
Address: Aero – Aircraft Design and Systems Group, Berliner Tor 9, 20099Hamburg, Germany

Abstract

This work studies the characteristics of the aerodynamics design of a box wing aircraft (BWA) with the potential gain of aerodynamics efficiency. The first objective of this paper is to study how BWA planform geometric parameters affect the aerodynamics efficiency. This is carried out using literature data and vortex lattice program. The second objective is to compare aerodynamics efficiency between BWA and conventional mid-range market aircraft. These comparisons are done considering trimming, Reynolds number variation and two types of airfoils.

Nomenclature

AOA	Angle of Attack
AVL	Athena Vortex Lattice
AR	Aspect Ratio
b	Aircraft span
BWA	Box Wing Aircraft
CA	Conventional Aircraft
C_D	Drag coefficient
C_{D0}	Zero-lift drag coefficient
C_L	Lift coefficient
$C_{L,ME}$	Lift coefficient for maximum aerodynamics efficiency
$C_{L,ME[BWA]}$	Lift coefficient for maximum aerodynamics efficiency of Box Wing Aircraft
$C_{L,ME[CA]}$	Lift coefficient for maximum aerodynamics efficiency of Conventional Aircraft
$D_{I,BW}$	Induced drag of a box wing
$D_{I,CW}$	Induced drag of a conventional wing
e	Oswald coefficient
E_{BWA}	Aerodynamics efficiency of Box Wing Aircraft
E_{CA}	Aerodynamics efficiency of Box Wing Aircraft
h	Gap. Height between BWA wings
h/b	Gap to span ratio
C_L / C_D	Aerodynamic Efficiency
M	Mach Number
NACA	National Advisory Committee for Aeronautics
NASA	National Aeronautics and Space Administration
Re	Reynolds Number
Re_{BWA}	Reynolds Number for Box Wing Aircraft flight
Re_{CA}	Reynolds Number for Conventional Aircraft flight
V_{cruise}	Cruise speed
V_{ME}	Speed of maximum efficiency
λ	Lambda. Wing taper ratio

DOI: 10.13009/EUCASS2017-447

1. Introduction

The aeronautical industry has been facing significant economic and environmental challenges. To accomplish new market and regulation requirements, the aeronautical engineers are putting efforts in developing new propulsion systems such as more efficient turbines and electric propulsion. Besides, non-conventional aircraft configurations could improve the aerodynamics efficiency substantially as well. The box wing aircraft (BWA) configuration presents an arrangement that increases the aerodynamics efficiency due to its potential lower induced drag and, therefore, lower fuel consumption. However, there are many design aspects that need to be evaluated to propose a BWA configuration as feasible design solution.

Torenbeek [1] presents a classification for airplane configurations. One of the categories is the nonplanar lifting system (also known as nonplanar wings) and single body. BWA belongs to this category. It is an airplane which its fuselage is similar to a conventional aircraft (CA) and its lifting system consists of two wings and there is not a horizontal tail. Front wing is aft-swept and rear one is forward-swept. Both wings have their tips connected by vertical fins, see figure 1. Together flying wings, nonplanar wings are being studied as alternative to increase aircraft performance.

Figure 1: Box wing aircraft model developed by AERO - Hamburg University of Applied Sciences. [2]

Lange et al [3] have studied a BWA for 400 passengers and cruise speed equal to Mach 0.95. They have not achieved the required flutter limit speed due to the low wing stiffness. To overcome this aeroelastic limitation, the penalty of shortening the vertical fins and increasing the aircraft weight have decreased the aircraft performance below an equivalent CA. Gallman [4] and Wolkovitch [5] have researched joined-wing aircrafts (JWA), it is similar to BWA but favors structural aspects once that the length of the vertical fins is zero. Gallman [4] has studied this type of aircraft and has achieved that JWA performance is inferior to CA because additional weight is necessary to comply with buckling requirement of the wing structure.

Frediani [6] has studied the relation between the induced drag of box wing divided by the induced drag of a conventional wing and gap to span ratio (*h/b*). Schiktanz and Scholz [2], [7] investigated a short-medium range BWA design and compared it against a CA. The BWA aerodynamics lead to a better glide ratio, but the BWA is much heavier, due to heavy wings. This leads to more induced drag and more fuel mass compared to the CA. Finally, also the Direct Operating Costs are higher. Longitudinal stability can be achieved also with a BWA, but CG travel is limited. The available fuel volume in the wings does not match requirements. For this reason, additional fuel tanks in the cargo compartment are required. Stability concerns are also reported by Andrews and Perez [8]. They analysed a BWA regional jet.

By the BWA literature, it is possible to understand that there is a potential performance gain for box wing configurations when compared to current configurations. However, aerodynamics, flight mechanics and structural designs must be carefully balanced to avoid impediments. This paper studies aerodynamics effects of BWA geometric parameters and compares aerodynamics efficiency between BWA and conventional mid-range size aircraft.

2. Methodology

The methodology section is divided in two subsections. The first one explains how the box wing planform is modelled and evaluates effects of geometric variation in the aerodynamics. The second one deals with the comparisons that are carried out between BWA and CA planforms.

DOI: 10.13009/EUCASS2017-447

2.1 Parametric evaluation of box wing aerodynamics

This parametric study is carried out using Athena Vortex Lattice (AVL) code and the considered box wing geometry has zero sweep, dihedral and twist angles. A NACA 0012 airfoil is adopted to model the box wing. The airfoil drag polar data is obtained from the literature [9]. The reference wing is kept constant equal to 120 m² and for all cases, the rear and front wing geometries are equal.

Figure 2 helps to understand what means stagger and gap. The stagger is the distance in X axis direction between front and rear wings [7]. According Zyskowski [10] "The total induced drag of any multiplane lifting system is unaltered if any of the lifting elements are moved in the direction of the motion provided that the attitude of the elements is adjusted to maintain the same distribution of lift among them". This excerpt refers to Munk's theorem. Hence, once that this work will not study wing twist, the stagger effects cannot be evaluated once that twist is necessary to keep the wing loading constant for different values of stagger. However, it may be supposed that its effects in the induced drag would be small. When the stagger is increased, the tip fin wetted area increases as well. Then the aircraft viscous drag increases also. It means that if it is considered only aerodynamics aspects, the stagger should be minimized. Schirra et al [11] presents more details about stagger evaluation of a box wing using AVL.

From the literature [1, 6, 7] it is known that the *h/b* ratio is an important parameter for the BWA aerodynamic characteristics. Hence this parameter is chosen to be variated together with the aspect ratio and taper ratio. Once that the wing area is constant, the aspect ratio is resulted from chosen span values. The adopted range is based on typical mid-range market aircraft. The simulation test matrix is presented in table 1. As can be seen, there are 75 box wing geometries analysed.

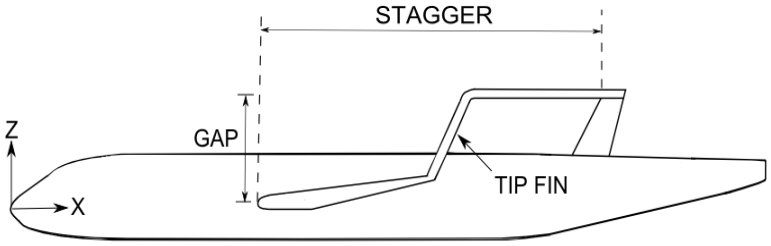

Figure 2: Key box wing geometric parameters.

Table 1: Numerical test matrix for box wing simulation

Parameter	Values
Aspect ratio	8.53 ; 9.63 ; 10.8
Taper ratio	0.2 ; 0.4 ; 0.6 ; 0.8 ; 1.0
Gap over span ratio (h/b)	0.1 ; 0.2 ; 0.3 ; 0.4 ; 0.5
Wing area	120 m²
Airfoil for wing and tip fins	NACA0012

Once defined the test matrix, the geometries modelled using AVL will be described. First of all, it is necessary to understand that it is not expected to have high fidelity results using vortex lattice methods. Reference [11] has raised limitations of the trailing wake modelling on the induced drag accuracy, for example. The goal of the analysis is to understand the aerodynamics behaviour. The test matrix is simulated with Mach number equal to zero. Then, they do not take account air compressibility effect. To estimate the viscous drag polar, Reynolds number is equal to ten million.

According the AVL's manual [12], the viscous drag is calculated from the two-dimensional airfoil drag polar. To obtain this data, the experimental data available in reference [9] is utilised. One observation about airfoil drag polar calculation consists in the fact that AVL allows the user to insert only one parabolic function for each airfoil. The experimental airfoil drag polar do not obey this function for higher lift coefficients. Then there is accuracy loss in this region.

The AVL modelling validation is carried out using two references. Goett and Bullivant [13] present results for wind tunnel tests for a wing (conventional wing) composed by NACA0012 airfoil and aspect ratio equal to six. The experimental procedure is carried out with Reynolds number equal to 3.3 million. These tests are simulated using AVL and the results are compared. The goal of this procedure is to evaluate if the viscous drag calculated by

DOI: 10.13009/EUCASS2017-447

the model is reasonable. The two-dimensional drag polar input in AVL is estimated from interpolation of the data available in reference [9].

The box wing model validation is carried out comparing its results with that presented by Prandtl [14]. In this case, only the induced drag can be compared. In his paper, Prandtl presents an approximated relation between induced drag of a conventional wing and a box wing with the same area and aspect ratio as function of the gap ratio, see equation (1).

$$\frac{D_{I,BW}}{D_{I,CW}} \approx \frac{1 + 0.45\left(\frac{h}{b}\right)}{1.04 + 2.81\left(\frac{h}{b}\right)} \tag{1}$$

Prandtl supposes that the wing loading distributions are elliptical. Then, the AVL conventional wing geometry that is utilised as reference has taper ratio equal to one and the aspect ratio is equal to two. Each AVL box wing configuration utilised for validation has also aspect ratio equal to two and taper ratio equal to one. The upper and lower wings of the box wing are equal and the sum of their areas is equal to the conventional wing area. Finally, the induced drag ratio is calculated from dividing the span efficiency factor calculated by AVL for the conventional wing by the same value for the box wing.

To minimize processing time, after the validation, a grosser panelling is adopted for execution of the tests described in table 1. Other limitations are related to the quantities of panels in chord and span directions. They are kept constant and, therefore, the mesh varies for each geometry. With the obtained results, graphics for induced, viscous and total drags for lifting coefficient equal to 0.5 as function of *h/b* ratio are utilised to describe the effects of the geometric parameters.

2.2 Aerodynamics comparison between BWA and CA planforms

Two planforms are evaluated in order to compare aerodynamic efficiency as function of lifting coefficient. Table 2 summarizes the main utilised parameters to describe the wing planform. When necessary, planform geometric data, close to data available in [7] and [15], are utilised as reference to represent a conventional aircraft. The taper ratio of BWA aircraft is obtained from the results of the analysis explained in section 2.1. Gap to span ratio is arbitrarily chosen because it would be result of structural analysis. Figure 3 presents both AVL aircraft models.

Table 2: Description of compared aircrafts

Parameter	Box wing aircraft	Conventional Aircraft
Wing and reference area	120.7 m²	120.7m²
Aspect ratio	9.58	9.58
Taper ratio	0.400	0.246
Wing twist angle	Zero	Zero
Incidence angle	Zero	Zero
Dihedral angle	Zero	Zero
Wing sweep angle (leading edge)	25º	25º
Tip fin sweep angle (leading edge)	25º	Not applicable
Gap to span ratio	0.138	Not applicable

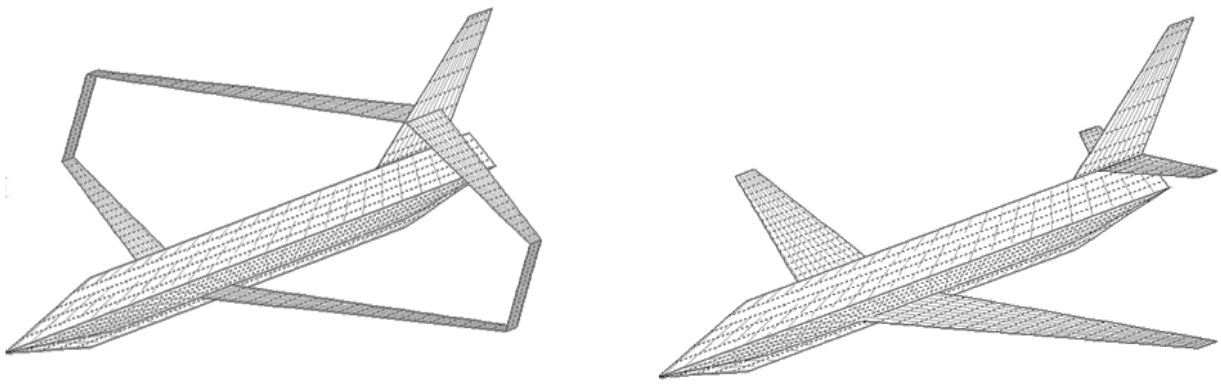

Figure 3. Images of the AVL models. BWA aircraft on the left and CA on the right.

DOI: 10.13009/EUCASS2017-447

The fuselage is modelled using a degenerated representation made by flat plate panels [16], including the area between wings and no viscous drag is associated to its panels. To estimates the aircraft total drag, this is divided in two parcels. The first one is the drag calculated by AVL, hence, it is the sum of the wing and empennages drag. The second parcel consists of the difference between total aircraft drag minus the first parcel. Reference [17] has a graphic for drag coefficient of regional narrow body airliners as function of Mach number and lift coefficient. Then the CA model is calculated for C_L = 0.5 and M = 0.7. The obtained value for the second parcel was 0.01278. This procedure contains some errors because the aircraft from reference and CA modelled using AVL, and all parameters of the flight condition are not equal, but this limitation was considered acceptable because the obtained value is utilised for both BWA and CA AVL models and to carry out comparisons between them. To allow trimming analysis, an elevator is modelled in each aircraft. It is positioned in the rear wing of BWA and has the same area of the correspondent CA. The placement of the centre of gravity is obtained from the calculated coordinate X of the aerodynamic neutral point of each aircraft at C_L = 0.5 and it is summed 20% of the reference chord.

To understand how the airfoil is modelled, it is necessary to expose the numerical test matrix for aircrafts planform comparisons, table 3. First, NACA0012 airfoils are applied with a drag polar at *Re* = 10.0 million and untrimmed condition. Second, because the chord of the BWA is half of CA (for viscous drag estimation proposals), the drag polar of CA wing is changed to be equivalent to *Re* = 20.0 million. Because it was not found an experimental data in the literature for this Reynolds number, it was utilised XFOIL data corrected by the closest test data from reference [9]. The third simulation case consists of the second case but in a trimmed condition. Finally, in the fourth test, it is applied supercritical SC(3)0712 airfoil in both aircrafts and a non-trimmed simulation is carried out. The drag polar of BWA considers *Re* = 15.0 million and CA considers *Re* = 30.0 million. The reference [18] contains the wind tunnel data. These Reynolds numbers are chosen because they have ratio equal to 0.5. The trimmed condition is not evaluated for configurations that have supercritical airfoils because the elevator design is not scope of this paper. To place an elevator in a surface that has the airfoil lifting coefficient equal to 0.7 would lead to further elevator design discussions.

Table 3. numerical test matrix for aircrafts planform comparisons

Test	**BWA Airfoil**	**CA Airfoil**	**Empennages and vertical fin airfoils**	**AVL Mach**	**Trimmed Condition**
1	NACA 0012, *Re* = 10.0E6	NACA 0012, *Re* = 10.0E6	NACA 0009, *Re* = 9.0E6	0.68	No
2	NACA 0012, *Re* = 10.0E6	NACA 0012, *Re* = 20.0E6	NACA 0009, *Re* = 9.0E6	0.68	No
3	NACA 0012, *Re* = 10.0E6	NACA 0012, *Re* = 20.0E6	NACA 0009, *Re* = 9.0E6	0.68	Yes
4	SC(3)0712, *Re* = 15.0E6	SC(3)0712, *Re* = 30.0E6	SC(2)0010, *Re* = 15.0E6	0.68	No

Regarding the empennages of both aircrafts and BWA tip fins, their airfoils are symmetrical. When the wing is simulated with NACA airfoils, NACA0009 airfoils are applied in these surfaces and its drag polar data is obtained for *Re* = 9.0 million from reference [19]. When the supercritical airfoil is utilised, the airfoil SC(2)0010 substitutes NACA0009 and its two-dimensional drag polar is calculated for *Re* = 15.0 million and it is obtained using XFOIL.

From the literature [20], the cruise lift coefficient is between lift coefficient for minimum drag and lift coefficient for maximum range. Considering that a lift coefficient value determines the cruise speed, it is possible to write V_{cruise}/V_{ME}. For aircraft optimization purposes, this speed ratio should be between 1 and 1.316. Then,

$$C_L = \frac{C_{L,ME}}{(V_{cruise}/V_{ME})^2} \tag{2}$$

and from a parabolic aircraft drag polar,

$$C_{L,ME} = (C_{D0}\pi ARe)^{0.5} \tag{3}$$

Supposing a design C_L = 0.5, it is checked if the aircraft are within the expected speed range and the ratio between them to evaluate if, from performance aspects, the aircrafts are compatible.

DOI: 10.13009/EUCASS2017-447

3 Results and discussion

3.1 Results for parametric evaluation of a box wing aerodynamics

Figure 4 presents the comparison between experimental results presented by Goett and Bullivant and obtained by AVL. The errors for figure 4a are lower than 2% and for figure 4b varies between -13% and -7%, the negative signal shows that the predicted drag is lower than experimental. The behaviour of both curves is similar to reference values. As expected, the lift curve, which for small AOA values, is dominated by potential flow, is accurate. This reflects in the correct induced drag and span efficiency factors predicted by AVL for box wing. As can be seen in figure 5, using the models built with AVL, values close to the given by equation (1), reference [14], have been obtained. Hence, the AVL modelling approach is considered valid for the purposes of the analysis carried out in this paper.

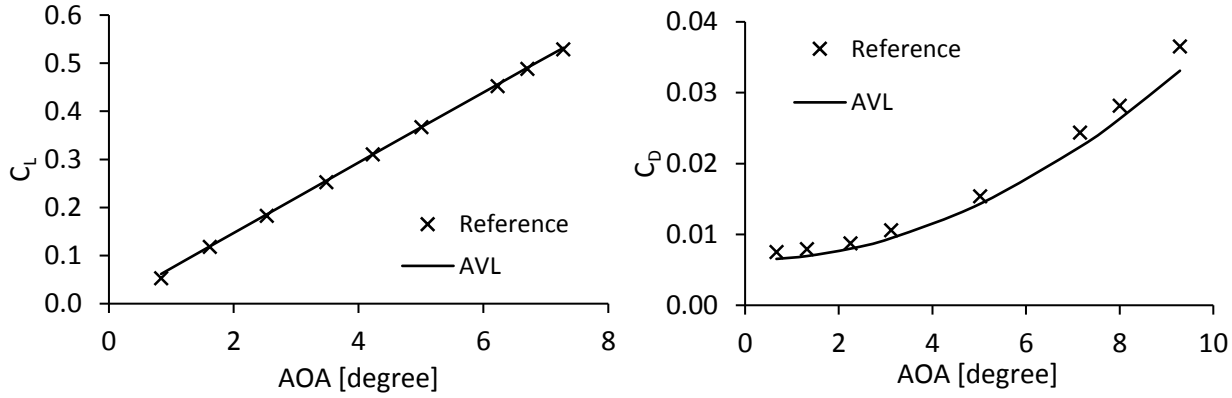

Figure 4. Comparison between AVL analysis and results from reference [13]. Figure 4a is C_L versus AOA and figure 4b is C_D versus AOA.

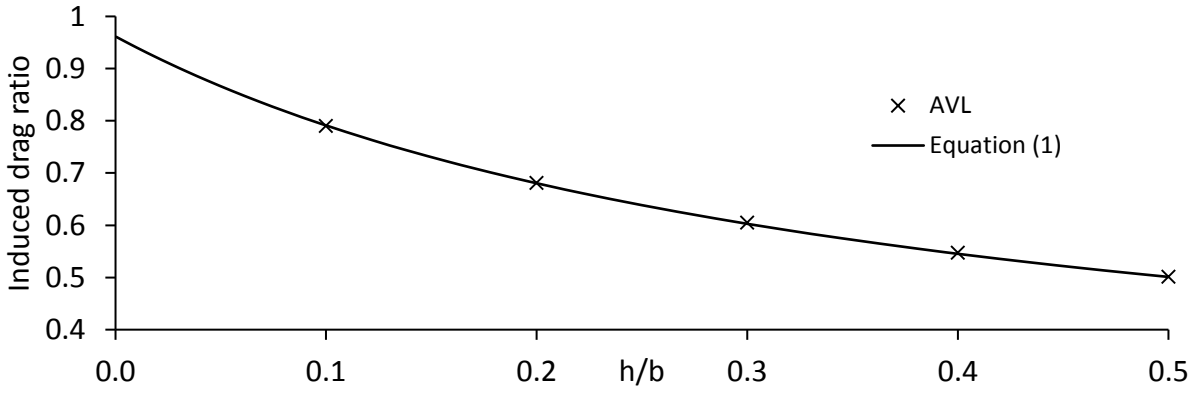

Figure 5. Comparison between box wing AVL results and equation (1) published by Prandtl [14].

Figure 6 presents the induced drag coefficient for $C_L = 0.5$. Results for all geometries are plotted. As can be seen, the aspect ratio is a major geometric parameter. It separates the results in three groups, each of them corresponds to one aspect ratio. Hence this behaviour is similar to the wing of a conventional aircraft. However, the influence of the gap to span ratio in the induced drag is as important as the aspect ratio for $h/b < 0.2$. The taper ratio effect varies with gap to span ratio. For lower values of h/b, it is similar to conventional aircraft. For $h/b = 0.1$, the lowest induced drag is between 0.4 and 0.6. However, when h/b is increased, it can be seen that higher taper ratios presents lower induced drag derivative, therefore their respective induced drags decrease faster. Considering gap to span ratio between 0.1 and 0.2, taper ratio equal to 0.6 is the best tested value.

The influence of the wetted area of the vertical fins, that depends of the respective airfoil drag polar, is shown in figure 7. As expected, when taper ratio increases, the wetted area of the vertical fin increases linearly. So, the viscous drag is a first-degree function for this simplified modelling. Actually, there is interference drag in this region as well. Only the data for aspect ratio equal to 9.63 is presented to facilitate the plot understanding.

DOI: 10.13009/EUCASS2017-447

When total drag is computed, Figure 8, the lower values of taper ratio present advantage in aerodynamic performance. Instead of higher induced drag, the lower viscous drag makes that λ = 0.4 is the best value for gap to span ratio between 0.1 and 0.2. For higher gap to span ratio values λ = 0.2, that was the worse value for the induced drag, is the best option for total drag. The effect of the gap to span ratio in the total drag is lower than in the induced drag.

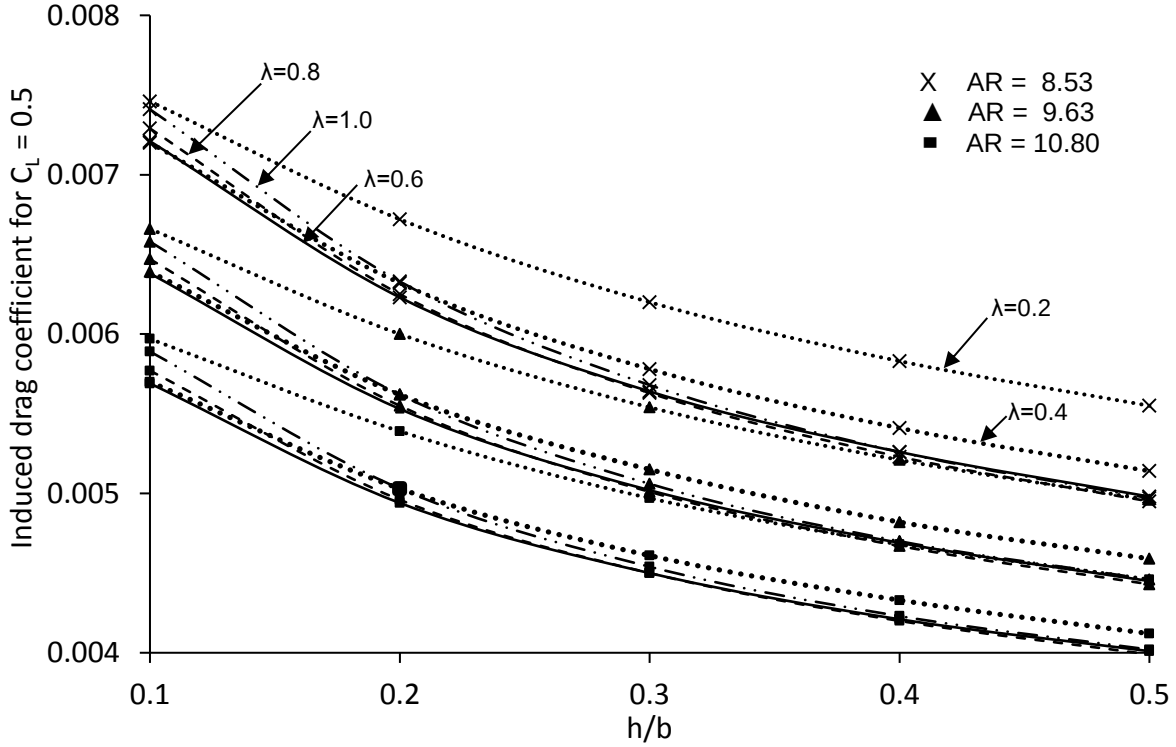

Figure 6. Obtained results for values from table 1. Induced drag for C_L = 0.5 versus *h/b*.

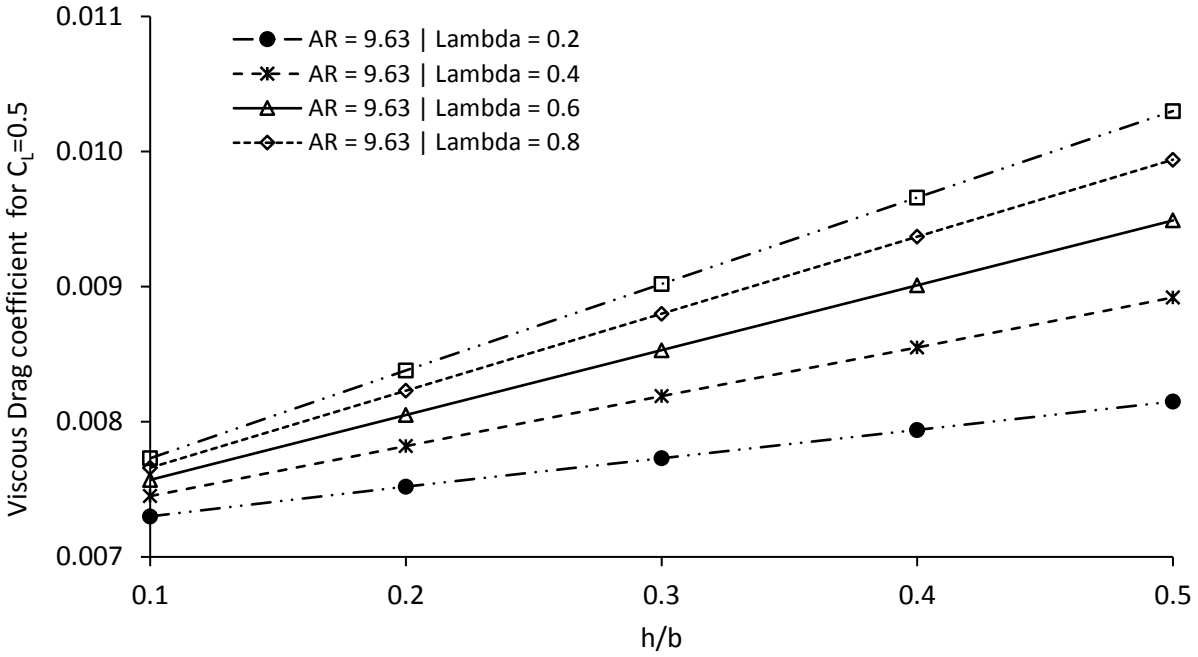

Figure 7. Obtained results for AR = 9.63 according table 1. Viscous drag for C_L = 0.5 versus *h/b*.

DOI: 10.13009/EUCASS2017-447

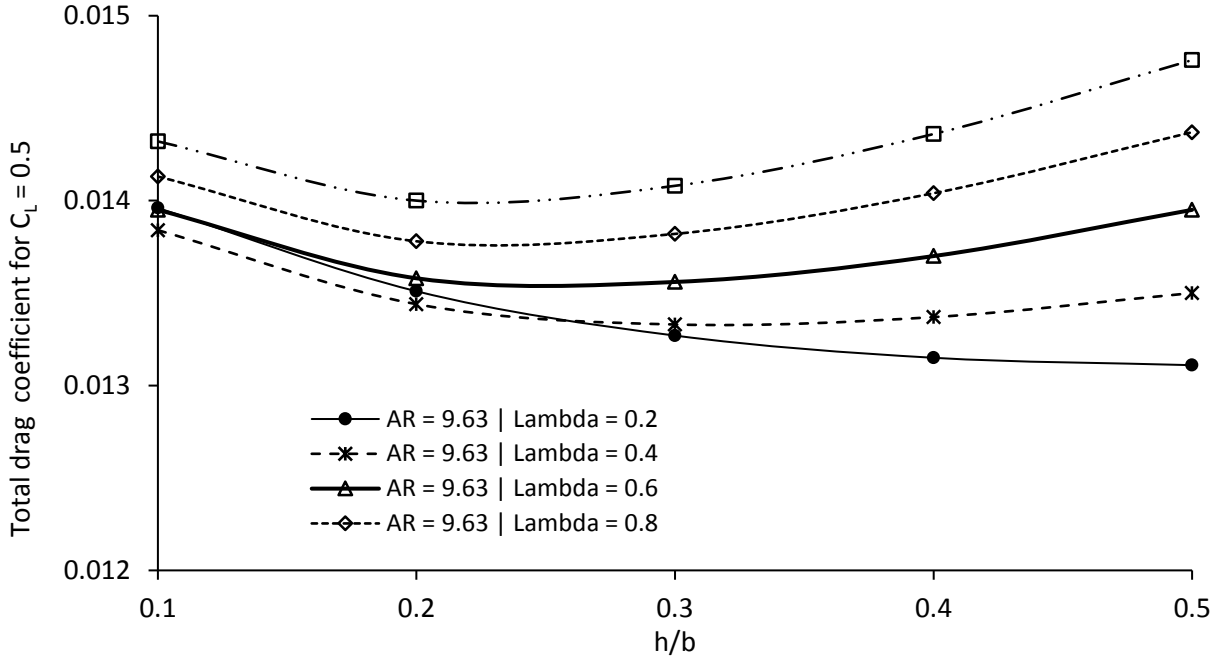

Figure 8. Obtained results for AR = 9.63 according table 1. Total drag for C_L = 0.5 versus *h/b*.

3.2 Results for planform comparisons

Figure 9 presents the results for test 1 described in table 3. As can be seen, with this setup, BWA aircraft is more efficient than CA for all values of lift coefficients. For C_L = 0.5, the efficiency ratio is 8.05%. For higher C_L values, the BWA can be up to 16.24% more efficient. From equation (3), $C_{L,ME}$[BWA] = 0.82 and $C_{L,ME}$[CA] = 0.73. Hence, because the Oswald values for BWA is higher than CA, the maximum aerodynamics efficiency of BWA occurs after than CA. The calculated speed ratio for BWA is 1.284 and for CA is 1.205, so 6.2% lower. The summary containing viscous drag for zero lift values and Oswald factors for all run cases is in table 4.

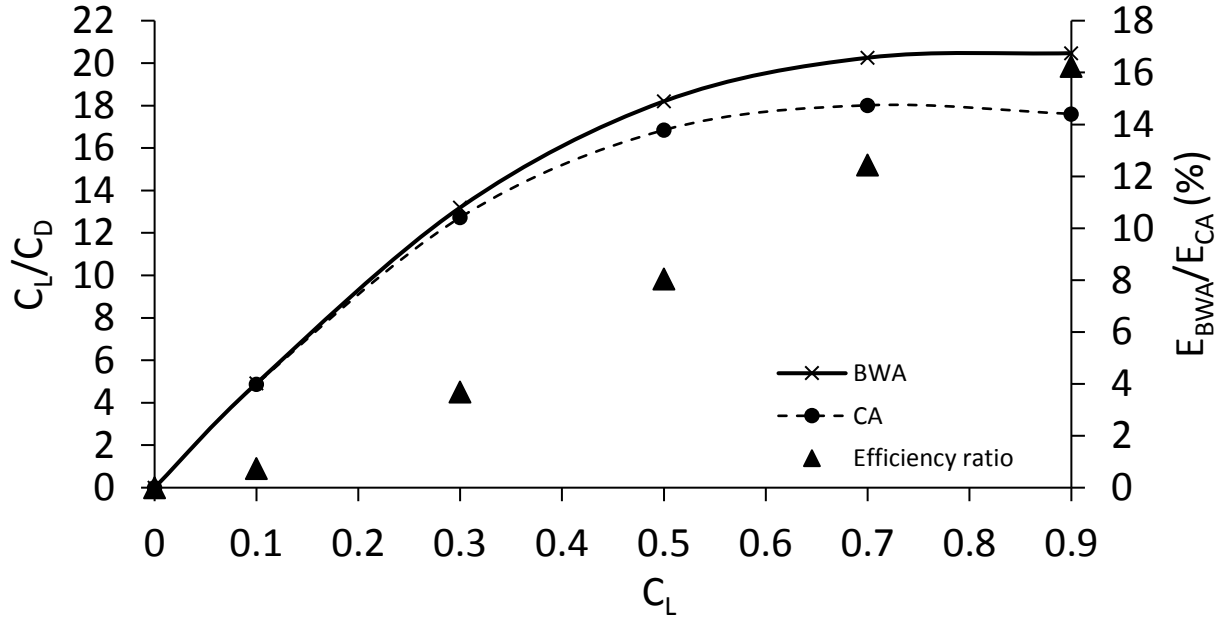

Figure 9. Comparison between BWA and CA planforms. Airfoils NACA0012. $Re_{BWA} = Re_{CA}$ = 10E6. No trim.

As said in section 2, for viscous drag estimation purposes, the BWA flies with Reynolds number equal to a half of CA. Then it is carried out the same analysis, but now the CA aircraft have its wing airfoil drag polar estimated with *Re* = 20E6. Figure 10 presents the results for test 2 described in table 3. BWA aircraft continues to be more

DOI: 10.13009/EUCASS2017-447

efficient than CA for all values of lift coefficients. But the difference decreases a bit. For C_L = 0.5, the efficiency ratio is 7.50%. For higher C_L values, the BWA can be up to 15.24% more efficient. It should be noted that for other Reynolds number values or other airfoils, the effect of flight Reynolds number may change.

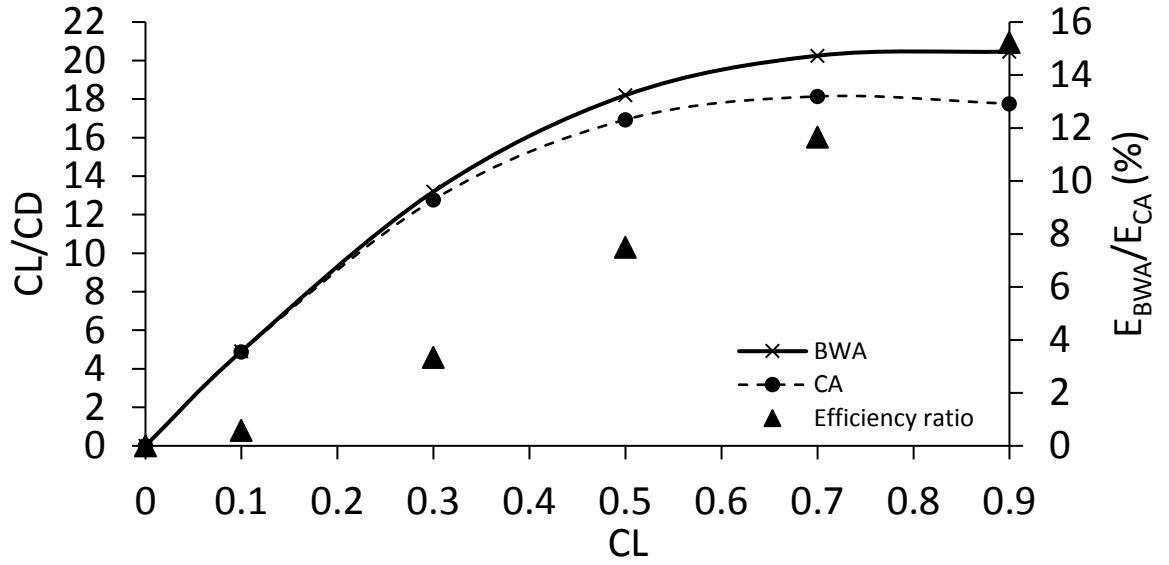

Figure 10. Comparison between BWA and CA planforms. Airfoils NACA0012. Re_{BWA} = 10E6 and Re_{CA} = 20E6. No trim.

Figure 11 presents the results for test 3 described in table 3. For this situation, the trimming has increased the BWA advantage. For C_L = 0.5, the efficiency ratio is 8.53%. For higher C_L values, the BWA can be up to 17.45% more efficient. Once that lever arm of BWA is smaller, its angle of elevator is higher than CA for cruise lift coefficient as shown by figure 12. The increased drag caused by higher angle of the elevator appears to be compensated by a better efficiency of the BWA for induced drag even with the rear wing being modified by the elevator. Further investigations are necessary about elevator design for BWA aircraft and how to model it.

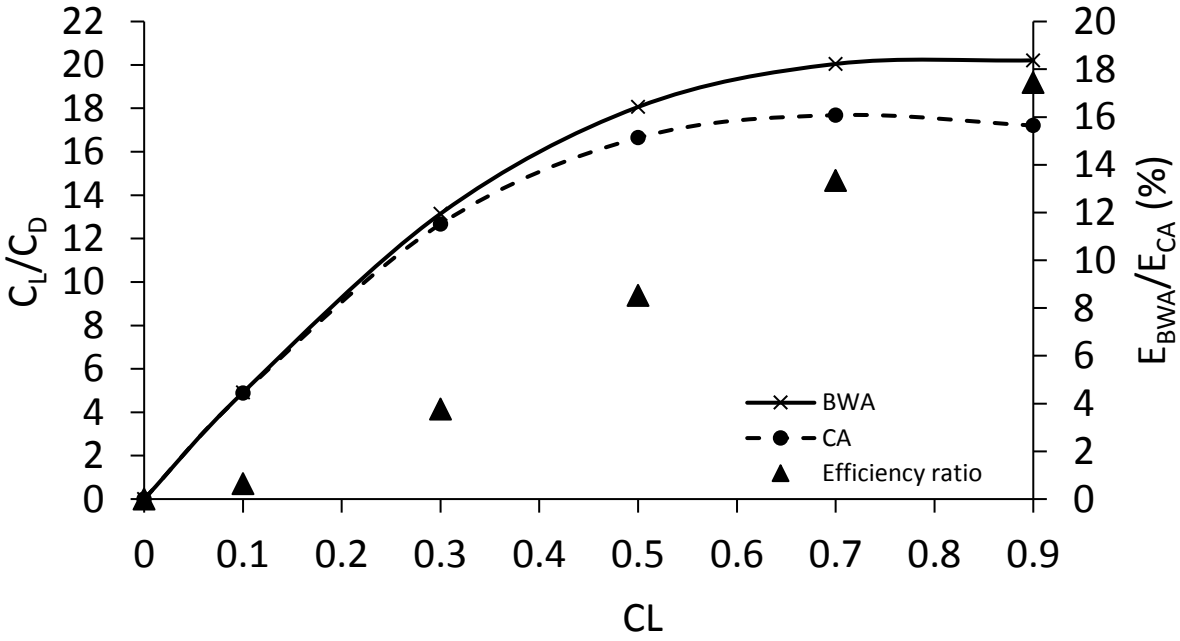

Figure 11. Comparison between BWA and CA planforms. Airfoils NACA0012. Re_{BWA} = 10E6 and Re_{CA} = 20E6. Trimmed.

DOI: 10.13009/EUCASS2017-447

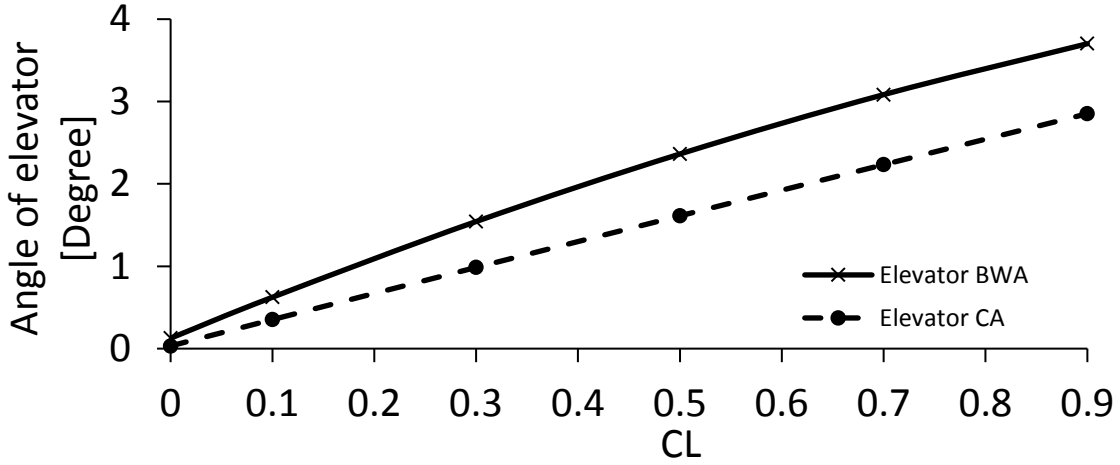

Figure 12. Comparison between BWA and CA elevator's command. Airfoils NACA0012. Re_{BWA} = 10E6 and Re_{CA} = 20E6. Trimmed.

The final comparison consists in the test number 4, Figure 13. Wings are configured with SC(3)0712 supercritical airfoil and empennages or vertical fins with SC(2)0010. The flight Reynolds numbers are increased for 15E6 and 30E6. Although the BWA is still more efficient, its advantage is the lowest among the tested cases. For C_L equal to 0.5, the efficiency ratio is 6.02%. The BWA advantage decreases because the aircraft viscous drag is increased for both aircrafts due to the changed airfoils, but this effect is stronger for BWA that has higher wing wetted area. Additionally, the lifting system of a BWA decreases only the induced drag. Once that the total drag for subsonic applications is given by the sum of induced and viscous drag, if viscous drag is increased for both aircrafts, the advantage of a BWA decreases.

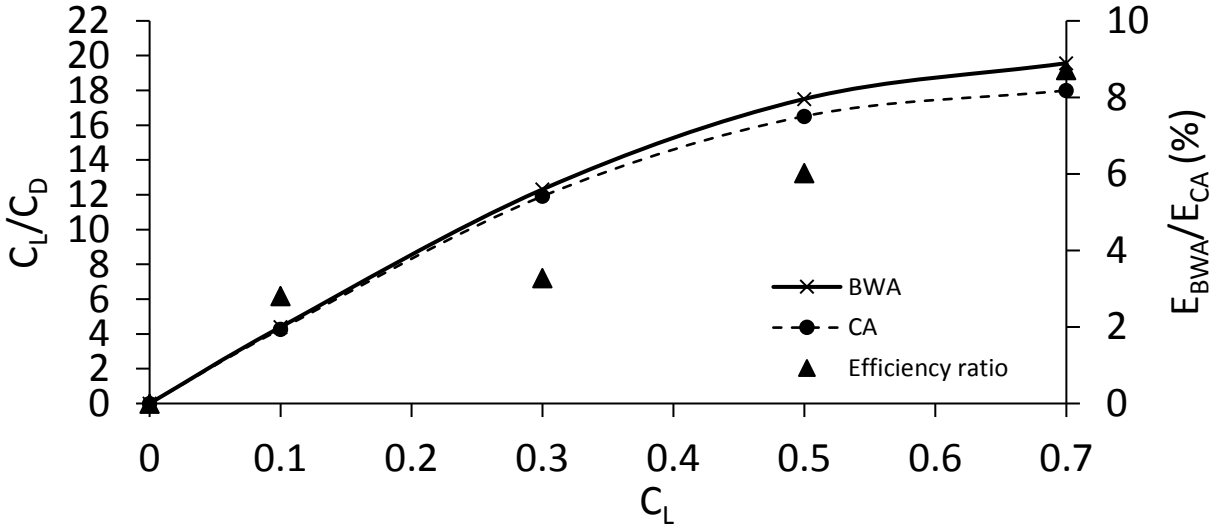

Figure 13. BWA and CA planforms comparison. Supercritical airfoils. Re_{BWA} = 15E6 and Re_{CA} = 30E6. No trim.

Table 4 presents results for tests 1, 2 and 3. Because the wing airfoil is symmetric, the two-term aircraft drag polar can be utilised to application of equations (2) and (3). As can be seen, once that BWA Oswald factors are higher than CA ones, the C_L values for maximum efficiency and the speed ratio are higher for BWA. Hence, for aerodynamics and performance comparisons purposes, it is better to do not fix cruise C_L, wing area and the airfoil at the same time. Reference [7] presents similar conclusion and suggests that the BWA could fly higher. Reference [21] indicates that BWA wing area may be smaller than CA one. It is interesting to note that although the reference areas are equal, the BWA wetted wing area is higher because the area near the vertical empennage is not covered by the aircraft fuselage. Another possibility would be to compare the planforms applying optima airfoils for each wing respectively. It means that both wings would have compatible values for $C_{L,ME}$, cruise speed ratio or relation between cruise efficiency and maximum efficiency. Because the airfoil of test 4 is not symmetric, the two-term drag polar is only an approximation. Then these analyses are not carried out.

DOI: 10.13009/EUCASS2017-447

Table 4. Summary data of two-term drag polar and results from application of equations (2) and (3).

	CD_0		Oswald factor		$C_{L,ME}$		Speed ratio (V_{cruise}/V_{ME})	
Test	**BWA**	**CA**	**BWA**	**CA**	**BWA**	**CA**	**BWA**	**CA**
1	0.02006	0.02013	1.1263	0.8698	0.82	0.73	1.284	1.205
2	0.02006	0.02010	1.1263	0.8813	0.82	0.73	1.284	1.208
3	0.02006	0.02010	1.1002	0.8348	0.82	0.71	1.227	1.192
4	0.02276	0.02517	-	-	-	-	-	-

4 Conclusions

From the parametric analysis, it is possible to conclude that the application of AVL program is adequate to understand the aerodynamics behaviour of a BWA. As expected from literature, aspect ratio and gap to span ratio are major geometric parameters. For $h/b < 0.2$, the gap to span ratio parameter is as important in the induced drag as the aspect ratio. Higher values of h/b offer less induced drag when taper ratio increases. However, the taper ratio increases the tip fin viscous drag. If $h/b < 0.2$, within the calculated values, the minimum total drag corresponds to a taper ratio value equal to 0.4.

Regarding the planform comparisons, the BWA have an aerodynamic efficiency higher than CA considering the adopted simplifications. The effects of Reynolds number and trimming were minor for the simulated cases. The BWA is sensitive to the increment of airfoil viscous drag because the modelled BWA wetted area is higher than CA aircraft. Also, aspects of aircraft performance should be taken in account to have a better comparison between the aircraft configurations.

References

[1] Torenbeek, E. 2013. Aircraft Design Optimization, in Advanced Aircraft Design: Conceptual Design, Analysis and Optimization of Subsonic Civil Airplanes, John Wiley & Sons, Ltd, Oxford, UK.

[2] Scholz, D. 2016. Evolutionary Aircraft Configurations – Possible A320 Successor. Research Project 2008-2014. – URL: http://Airport2030.ProfScholz.de

[3] Lange, R.H., J.F. Cahill, et al. 1974. “Feasibility Study of the Transonic Biplane Concept for Transport Aircraft Application”, NASA Contractor Report CR-132462.

[4] Gallman, J.W., S.C. Smith, and I.M. Kroo. 1993. “Optimization of Joined-Wing Aircraft”, Journal of Aircraft, Vol. 30, No. 6, pp. 897–905.

[5] Wolkovitch, J. 1986. “The Joined Wing: An Overview”, Journal of Aircraft, Vol. 23, No. 3, pp. 161–178. (also AIAA Paper No. 85–0274, 1985).

[6] Frediani, A., and Montanari, G. 2009. “Best wing system: an exact solution of the Prandtl’s problem,” Variational Analysis and Aerospace Engineering, Vol. 33.pp. 183-21.

[7] Schiktanz, D., and Scholz, D. 2011. “Box Wing Fundamentals – An Aircraft Design Perspective”, In: DGLR: Deutscher Luft- und Raumfahrtkongress 2011 : Tagungsband - Manuskripte (DLRK, Bremen, 27. - 29. September 2011), S. 601-615. - ISBN: 978-3-932182-74-X. DocumentID: 241353. Download: http://Airport2030.ProfScholz.de

[8] Andrews, S. A., and Perez, R. E.2015. "Multidisciplinary Analysis of a Box Wing Aircraft Designed for a Regional-Jet Mission", 16th AIAA/ISSMO Multidisciplinary Analysis and Optimization Conference, AIAA Aviation, 2015.

[9] Sheldahl, R. E., and Klimas, P. C. 1981. “Aerodynamic characteristics of seven airfoil sections through 180 degrees angle of attack for use in aerodynamic analysis of vertical axis wind turbines,” SAND80-2114, Albuquerque, NM.

[10] Zyskowski M. K. 1993. Incorporating biplane theory into a large, subsonic, all-cargo transport. A report prepared for the University Space Research Association, in Cooperation with the NASA Langley Research Center.

[11] Schirra J. C., Watmuff J. H. and Bauschat J. M. 2014. Accurate induced drag prediction for highly non-planar lifting systems. 19th Australasian Fluid Mechanics Conference. Melbourne, Australia.

[12] Drela, M., and Youngren, H. 2010. “AVL’s User Guide,” Massachusetts Institute of Technology.

[13] Goett, H. J., and Bullivant, W. K. 1939. “Tests of NACA 0009, 0012, and 0018 Airfoils in the Full-Scale Tunnel,” NACA TR-647.

DOI: 10.13009/EUCASS2017-447

[14] Prandtl L. 1924. Induced Drag of Multiplanes. Hampton: National Advisory Commitee for Aeronautics. NACA TN 182.
[15] Airbus, 2017. Autocad 3-view aircraft drawings. - URL: http://www.airbus.com/support-services/airport-operations/autocad-3-view-aircraft-drawings. Accessed 2017-06-13
[16] Belben J. B. 2013. Enabling rapid conceptual design using geometry- based multi-fidelity models in VSP. Msc Thesis. Faculty of California Polytechnic State University.
[17] Obert, E. 2009. Aerodynamic Design of Transport Aircraft. IOS Press.
[18] Johnson W. G., Jr., Hill A. S., and Eichmann O. 1985. High Reynolds Number Tests of a NASA SC(3)-0712(B) Airfoil in the Langley O.3-Meter Transonic Cryogenic Tunnel. NASA Technical Memorandum 86371.
[19] Abbott, I. H., and von Doenhoff, A. E. 1959. Theory of Wing Sections: Including a Summary of Airfoil Data, Dover Publications, Toronto.
[20] Scholz D. 2017. Aircraft Design Lecture Notes. Hamburg Open Online University. – URL: http://HOOU.ProfScholz.de
[21] Schiktanz, D., and Scholz, D. 2014. Maximum Glide Ratio of Box Wing Aircraft – Fundamental Considerations. Memo, Aircraft Design and Systems Group. URL: http://Reports-at-AERO.ProfScholz.de, PDF-Download: https://goo.gl/vV44MJ. Accessed 2017-05-10